Control of a Distributed Generation Unit Including PV-array, Hydrogen Unit and Battery Storage

M. Shirazi, M. R. Zolghadri, H. Karimi, and M. Popov

Abstract—**This paper presents a control strategy for the stand-alone operation of a distributed generation (DG) unit. The DG unit consists of a photovoltaic (PV) array as a primary source of energy, a hydrogen unit as a long-term storage system, and a battery as a short-term storage device. The hydrogen unit itself includes a fuel cell (FC) and electrolyzer. The DG system supplies a three-phase balanced load using a voltage-sourced converter (VSC). The PV-array, the battery, the FC, and the electrolyzer are connected to the DC link of the VSC through DC-DC converters. The control strategy of the DG unit comprises two main control systems; a DC side and an AC side control system which can be assumed almost decoupled. The DC side controller is composed of four control subsystems associated with each DC-DC converter and a supervisory controller which determines the operating mode of the control subsystems. The supervisory controller manages the power flow between the DG units and the load. The AC side controller regulates the magnitude of the load voltage. The performance of the proposed control system is verified by MATLAB/Simulink in various operational scenarios.**

Keywords: **DG, Stand-alone, Photovoltaic, Hydrogen unit, VSC, DC-DC converter, Power management, DC link**

I. INTRODUCTION

Because of the depletable nature and daily increasing costs of fossil fuels, it seems that replacing the fossil fuels by another source of energy is inevitable. Moreover, in the remote areas where the electricity network is not accessible, using the renewable energy resources can be a good solution. Wind and solar energy have the greatest proportion of energy production among the renewable energy sources. However, there are several reasons for using solar energy rather than other sources of sustainable energies. For instance, the solar irradiance is ubiquitous. Moreover, solar energy system has no moving parts, low maintenance cost, and quiet operation. Nonetheless, it has some drawbacks such as high initial investment cost, low efficiency, and intermittent nature[1].

In remote areas where power grid is not accessible, solar energy could be used as a main source of energy. Due to the fluctuated characteristic of the solar radiant during a day, it is necessary to use another source of energy to guarantee the continuous supply of the load. According to [2],[3] applying the battery storage may be the simplest solution to overcome the fluctuate nature of solar energy. Nevertheless, battery has low energy density, large size and weight for a given capacity and voltage, and environmentally unfriendly nature. In [4] the battery is connected to a DC link directly. In this configuration, inrush currents caused by a sudden change of the power of the PV-array or load can damage the battery. Various hybrid DG systems are put forwarded in [2],[5]. In [2] the DC link voltage is lower than the PV-array voltage, so a buck converter is applied to connect the PV-array to the DC link. In [5], the energy sources are joined together through an AC link, even though this paper utilizes a DC link and decreases the number of interfaced converters.

In this paper, a stand-alone operation of a DG unit using PV-array as a primary source of energy is considered. In order to utilize the greatest potential of the solar energy and to decrease the battery capacity, a hydrogen unit is employed as a long-term storage system to save the exceeding generated power of the PV-array with respect to the load demand and to provide the shortage of power as well. Because of the slow dynamic of the fuel cell (FC), the battery storage device provides a balance between the transient power flow the sources and the load. The DC link divides the DG system in two parts: a DC- and an AC side system. The PV-array is connected to the DC link over a boost converter. Similarly, another boost converter connects the FC to the DC link. The DC link is connected to the electrolyzer by a buck converter. Since the battery should be able to be charged and discharged, a bidirectional DC-DC converter is used as an interface between the battery and the DC link. Each DC-DC converter has its own controller which can operate in various modes. A supervisory controller at the DC side determines the operating modes of each DC-DC converter controller. The operating modes of each converter are defined based on the generated power of the PV-array, the status of the battery, and the load demand. AC side system makes use of a VSC to connect a DC link to the load. The AC side controller regulates the load voltage magnitude. In this paper the DC link voltage, which is dictated by a desirable load voltage is higher than the PV-array voltage. Therefore, a boost converter is used as an interface between the PV-array and the DC link. The input inductor of the boost converter prevents the sharp change of the PV-array current.

This paper is organized as follows. The study system is described in chapter II. The models of DC side components and the AC side model are reported in chapters III and IV. The control strategy of the system is described in chapter V. The chapter VI presents the simulation results and conclusions are

M.Shirazi and H. Karimi are with the Sharif University of Technology Department of Electrical Engineering, Teheran, Iran
(e-mail: moein_shirazi@ee.sharif.ir ,houshang.karimi@sharif.edu).
M.R. Zolghadri is with Sharif University of Technology, Center of Excellent in Power Management & Control, Teheran, Iran
(e-mail: zolghadr@sharif.edu)
M. Popov is with Delft University of Technology, Department of EEMCS, Mekelweg 4, 2628CD, Delft, The Netherlands
(e-mail: M.Popov@tudelft.nl)

presented in chapter VII.

II. STUDY SYSTEM

Fig. 1 shows a schematic diagram of the proposed system. The PV-array is the main source for the DG unit whereas the battery and the hydrogen unit are used as storage system. A DC-DC converter is used to couple each energy unit to the DC link, the supervisory controller and the controller of each storage system. The DC-DC converter provides a constant voltage at the DC link. The AC side controller, which is assumed to be decoupled from the DC side controllers, regulates the load voltage magnitude. The load is modeled by a 20 kW passive balanced RLC network. A parallel RLC circuit is conventionally adopted as a local load for the evaluation of islanding detection methods when the inductance and capacitance of the load are tuned to the system frequency (60 Hz) [6]. The system parameters are summarized in Table I.

III. MODELING OF DC SIDE SYSTEM

This section presents mathematical models for the PV-array, battery storage, electrolyzer, and FC. Small signal AC models for DC-DC converters are reported.

A. PV-array

The solar cell converts the solar energy to electrical energy directly. The output voltage of a typical solar cell is between 0.6 V and 1 V. Therefore, several cells connected in series construct a PV-module to obtain a higher voltage. Similarly, the modules are connected together in series and parallel configuration providing a PV-array with the desirable voltage and output power.

Equation (1) shows the relationship between the voltage and the current of a PV- array

$$I = N_P I_{PH} - N_P I_s [e^{\frac{q(\frac{V}{N_s} + \frac{IR_s}{N_p})}{KT_c n}} - 1] - \frac{\frac{N_p V}{N_s} + IR_s}{R_{SH}} \quad (1)$$

In (1), I and V are the output current and the output voltage of the PV-array, N_s and N_p are the number of series and parallel cells, R_S, R_{SH} are the series and parallel resistances of the solar cell, respectively, q is the electron charge, K is the Boltzmann constant, and n is an ideal factor of the diode in the equivalent circuit which is between 1 and 2. Moreover, T_c and I_{PH} are the cell temperature in Celsius and the photocurrent of the solar cell, respectively [7]. The open-circuit voltage (V_{oc}), the short-circuit current (I_{sc}), the voltage (V_m) and current (I_m) of a module at the maximum power point, for the certain temperature and insolation, are given in the module datasheet.

This paper makes a use of the mathematical model of the PV-cell which is reported in [8]. The three basic equations of the mathematical PV-cell model are

$$I = I_{sc}(1 - C_1(e^{\frac{V}{C_2 V_{oc}}} - 1)) \quad (2)$$

$$C_2 = \frac{(\frac{V_m}{V_{oc}} - 1)}{Ln(1 - \frac{I_m}{I_{sc}})} \quad (3)$$

$$C_1 = (1 - \frac{I_m}{I_{sc}})e^{\frac{-V_m}{C_2 V_{oc}}} \quad (4)$$

In which I and V are the output current and the voltage of the PV-cell. Output characteristics of a PV-array depend on the insolation level and the ambient temperature.

In terms of the temperature and insolation, V_{oc}, I_{sc}, V_m, I_m of PV-cell are obtained as follows:

$$\Delta s = \frac{s}{S_{ref}} - 1 \quad (5)$$

$$I'_{sc} = I_{sc} \frac{s}{S_{ref}}(1 + a\Delta T) \quad (6)$$

$$V'_{oc} = V_{oc}(1 + c\Delta T[Ln(1 + b\Delta s])) \quad (7)$$

$$I'_m = I_m \frac{s}{S_{ref}}(1 + a\Delta T) \quad (8)$$

$$V'_m = V_m(1 + c\Delta T[Ln(1 + b\Delta s]) \quad (9)$$

Where S is the solar insolation (w/m²), S_{ref} is the reference insolation (1000 w/m²) and a, b and c are constants. ΔT is the error between the ambient temperature and the reference temperature (30ºC).

TABLE I   STUDY SYSTEM PARAMETERS

Load	R(Ω)	7.26
	L(H)	0.0107
	C(µF)	657.67
	R_L(resistance of inductor(Ω))	0.4
	Rated peak voltage(v)	220
	Frequency(Hz)	60
PV-array	Peak power(kW)	26
	Output voltage(v)	410-600
Battery	Rated voltage/capacity(v/Ah)	345/0.1
	$V_{bat,max}$ over charge voltage(v)	365
	$V_{bat,min}$ over discharge voltage(v)	320
	Fuel cell capacity(kW)	20
	electrolyzer capacity(kW)	12
	Time period of study(sec)	220
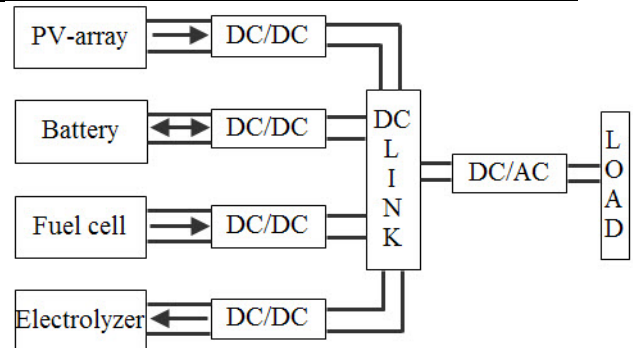
Figure 1   System configuration

The temperature, the insolation, and the output current of the PV-array are inputs of the PV model whilst the voltage and the power are its outputs.

B. Battery storage

This paper used the mathematical model of the lead acid battery which is described in [9]. Equations (10), (11) show the relationship between the battery current, the battery voltage, and the state of the charge of the battery (*SOC*). It is supposed that the charge current of the battery is negative.

$$V_B = E_0 + b \log(SOC) + R_B I_B \tag{10}$$

$$R_B = r_1 + r_2(SOC) + [r_3 - r_4(SOC)]^{-1} \tag{11}$$

where V_B is the output voltage of the battery, E_0 is the voltage of the battery at full charge state, R_B is an internal impedance, I_B is the battery current, and b, r_1, r_2, r_3, r_4 are empirical constants.

C. Fuel cell

FC is an energy conversion device that directly converts chemical energy to electrical energy by means of hydrogen and oxygen as fuel whereas the water and the heat are two secondary products of the FC. Solid oxide FC (SOFC) and proton-exchange membrane (PEM) are two types of FCs which are used in DG. Low temperature PEM which is described in [10] is used in this paper as a DG source, which is compact and has low weight. The detailed model of the FC expound in [11]. It is not efficient to start up the FC in below 15% of its rated power. Fig. 2 shows the polarization curve of FC. As it can be seen, it is divided in three zones: A voltage drop in the low current region because of the activation loss in FC, a linear voltage drop in the middle current region because of the ohmic losses in the FC associated with the internal resistance of the FC stack, and a drastically voltage drop at higher current region because of mass transfer over potential, which is associated with the sluggishness of mass transfer processes [13],[14]. The response time of the FC is assumed to be 3s to consider the dynamics of the FC.

The FC should be able to supply the load individually when the output power of the PV-array is zero, e.g. during the night. Based on the load demand, the FC capacity is assumed to be 20 kW.

D. Electrolyzer

An electrolyzer is a device that uses electricity to produce hydrogen and oxygen from water. In other words, the reaction in the electrolyzer is reverse of the FC reaction. The hydrogen produced by the electrolyzer is used as fuel by the FC. The details of the difference between the hydrogen produced by the electrolyzer and the hydrogen that is consumed by the FC is described in [15]. The electrolyzer can be considered as a nonlinear DC load. The amount of hydrogen is increased by increasing the DC voltage. Equation (12) expresses the relationship between voltage and current of an electrolyzer [16].

$$U = U_{ref} + (\frac{r_1 + r_2 T}{A})I + sLog(\frac{t_1 + \dfrac{t_2}{T} + \dfrac{t_3}{T^2}}{A}I + 1) \tag{12}$$

Where U_{ref} is the reversal voltage, T is the cell temperature expressed in Celsius, A is the electrode's area in square meters and I, U are the current and the voltage of the electrolyzer respectively [16].

The capacity of the electrolyzer is determined by the amount of exceeding generated power of the PV-array with respect to the load. Considering the maximum power generated by the PV-array and the load demand, a 6kW electrolyzer is used in this study.

E. DC-DC converters

A boost converter connects the PV-array and the FC to the DC link whereas a bidirectional converter, as shown in Fig. 3, connects the battery and the DC link. Moreover, DC link connected to the electrolyzer through a buck converter. The small signal AC model of the DC-DC converter is used to reduce the run-time of the simulation. The small signal model of the converter is discussed in [17]. If as much as the small signal model is proposed for continuous conduction mode (CCM) of the converter, it could be used for bidirectional converter.

IV. MODELING OF AC SIDE SYSTEM

To simplify the study of the AC side system, it is assumed that the DC link of the VSC has constant voltage. As Fig. 4 shows, a three-phase VSC is applied to convert the DC voltage to a set of balanced three-phase voltages. The AC side controller receives the output voltage and compares its magnitude to the reference voltage and then applies the error signal to produce the modulation signals for the VSC [6].

An internal oscillator is used for the regulation of the load voltage frequency in an open-loop manner. The mathematical model of the system and the control design procedure are expounded in [6].
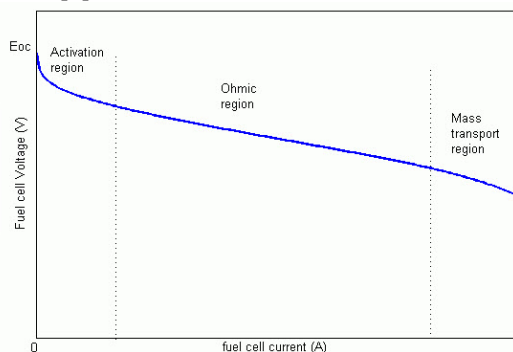
Figure 2   Polarization curve of fuel cell [12]
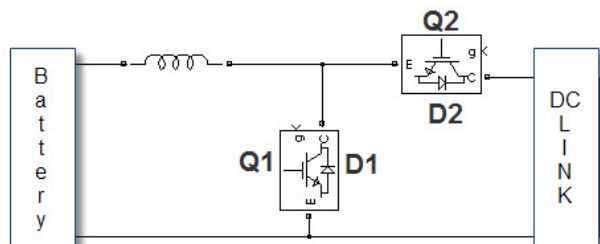
Figure 3   Bidirectional converter
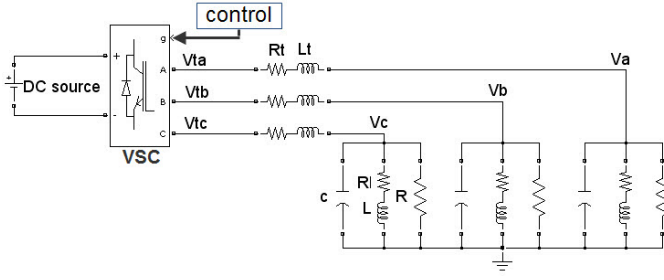
Figure 4   AC side configuration

The system model is defined by

$$X' = AX(t) + BU(t) \tag{13}$$

$$Y(t) = CX(t) \tag{14}$$

$$u(t) = v_{td} \tag{15}$$

Where A, B, C, X are

$$A = \begin{pmatrix} -\dfrac{R_t}{L_t} & \omega_o & 0 & \dfrac{1}{L_t} \\[2mm] \omega_o & -\dfrac{R_L}{L} & -2\omega_o & \dfrac{R_L C \omega_o}{L} - \dfrac{\omega_o}{R} \\[2mm] 0 & \omega_o & -\dfrac{R_L}{L} & \dfrac{1}{L} - \omega_o^2 C \\[2mm] \dfrac{1}{C} & 0 & -\dfrac{1}{C} & -\dfrac{1}{RC} \end{pmatrix}$$

$$B = \begin{pmatrix} \dfrac{1}{L_t} \\[2mm] 0 \\ 0 \\ 0 \end{pmatrix}, X = \begin{pmatrix} i_{td} \\ i_{tq} \\ i_{Ld} \\ V_d \end{pmatrix}, C = \begin{pmatrix} 0 & 0 & 0 & 1 \end{pmatrix}$$

where ω_0 is the AC system frequency, i_{td}, i_{tq}, i_{Ld}, and V_d, are individual phase quantities in dq frame.

The obtained controller for the VSC (C_{VSC}) is

$$C_{vsc} = \frac{8000}{s(s+150)}$$

The values of R_t and L_t represent the series filter and are 0.0015Ω and 0.003H, respectively.

V. POWER MANAGEMENT STRATEGY

The DC side control system comprises of a supervisory controller and four sub controllers which has two principle goals; to regulate the DC link voltage at a desirable constant level and to implement a proper power management by DC-DC converters to guarantee the continuous supply of the load.

Since the PV-array voltage is lower than the DC link voltage, a boost converter is used to connect the PV-array to the DC link. It is desired to utilize the extreme potential of the solar energy, so the PV-array should operate in its maximum power point in various environmental conditions. By the way, if there is not enough insolation e.g. in shaded condition or during the night, the PV-array should be shut down. Therefore, the boost converter of the PV-array operates in two modes. The supervisory controller takes the voltage of the PV-array and determines the operating mode of the PV-array boost controller. When the voltage of the PV-array is lower than a certain minimum value ($V_{PV,min}$), then the boost controller opens the switch of the boost converter, so the negative voltage is imposed to the boost inductor. The inductor current starts to decrease until it reaches current zero and the diode of the boost converter is turned off. When the PV-array voltage is higher than the $V_{PV,min}$, then the supervisory controller commands the boost controller to operate in a maximum power point tracking (MPPT) mode. A perturb and observe algorithm is employed for the MPPT because of its simplicity and easiness to use [1].

Based on the output power of the PV-array, the status of the battery, and the load demand, the DG unit operates in various operating modes.

A. Mode-1

When the output power of the PV-array is higher than the load demand and the battery voltage is lower than a certain maximum value ($V_{bat,max}$), the supervisory controller disables the FC and the electrolyzer converter, and it enables the controller of the bidirectional converter, so the battery is being charged by receiving the exceeding generated power of the PV-array with respect to the load demand. In this mode the bidirectional converter maintains the voltage of the DC link at a desirable constant value.

B. Mode-2

When the generated power of the PV-array is higher than the load demand and the battery voltage is not lower than $V_{bat,max}$, the supervisory controller enables the controller of the electrolyzer converter and disables the controller of the bidirectional and the FC converter. Therefore, the electrolyzer takes the exceeding generated power and it produces hydrogen.

C. Mode-3

In this mode the battery voltage is higher than a certain minimum value ($V_{bat,min}$) and the generated power of the PV-array is lower than the load demand as the difference of the power is lower than the 15% of the rated power of the FC. In this case, the supervisory controller disables the FC and the electrolyzer converts and enables the bidirectional converter. Therefore, the battery provides the shortage of the power.

D. Mode-4

This mode occurs when the mode-3 persists for long time so that the battery voltage is decreased and reaches the $V_{bat,min}$. At this state the supervisory controller sends commands to the controller of the bidirectional converter to segregate the battery from the DC link. It also sends an enabling command to the controller of the FC converter. In this state, the FC maintains the DC link voltage.

E. Mode-5

When the load demand is higher than the output power of the PV-array and the difference is higher than 15% rated power of the FC, the supervisory controller enables the FC converter and disables the electrolyzer and battery converters.

Considering the dynamic of the fuel cell the disabling command of the bidirectional converter should be sent with a delay to maintain the DC link voltage.

F. Mode-6

When the PV-array is separated from the system due to lack of the insolation, the FC supplies the load individually.

VI. SIMULATION RESULTS

The performance of the proposed DG unit system is verified by two different scenarios in the MATLAB/Simulink. In all scenarios the ambient temperature is assumed to be 25ºC and the PV-array operates at MPPT mode.

A. Scenario I

In this scenario the system operates in the normal operation. The pattern of solar insolation is shown in Fig. 5(a). Fig. 5(b) shows the balance of the power flow between DG units. Before t_1=39.82s, the FC compensates the shortage of the power and the battery and electrolyzer is segregated from the system. After t_1, the difference of the load demand and the generated power of the PV-array, reaches below 3kW and supervisory controller sends enabling command to the bidirectional controller and disabling command to the FC converter. So the battery is discharged and provides the lack of power until t_2=48.72s when the power of the PV-array being more than the load demand. From t_2 to t_3=71.01s the battery is being charged by taking the exceeding power. At t_3 the battery voltage reaches $V_{bat,max}$, so the supervisory controller enables electrolyzer converter and commands to separate the battery from the system. Therefore, from t_3 to t_4=191.27s the electrolyzer takes the exceeding power. After t_4 the power of the PV-array goes below 20kW and the battery is connected to the system again and provides the lack of power. This state persists until the output power of PV-array reaches below 17kW at t_5=200.17sec. After t_5 the FC the PV-array and the FC supply the load. Fig. 5(c) shows the operating mode of the system. The status of the battery is illustrated in Fig. 5(d). Constant level of the SOC implies the time that battery segregate from the system. Fig. 5(e) illustrates that, although coupling or decoupling of each unit to the DC link imposes a shock on its voltage, the controllers of DC-DC converters maintain the DC link voltage. Fig. 5(f) shows that the voltage of one phase of the load in the vicinity of t_1 when the mode change occurs. It is illustrated that the VSC controller regulates the load voltage magnitude properly.

B. Scenario II

This scenario verifies the performance of the system when load change occurs. The insolation level and the generated power of the PV-array are similar to scenario *I*. At t=42s the system is imposed to a step load change and the load demand being 0.75 of its initial value (15kW). Fig. 6 shows the response of the system to a load change.

Fig. 6(a) shows the power flow between DG units. The operating modes of the system and the status of the battery are shown in Fig. 6(b),(c). As it is shown in Fig. 6(a), the system operates in a similar manner to the scenario I until the load

change at t_2=42s takes place. After t_1=39.82s, the battery is being discharged to provide the shortage of power. But at t_2, the load demand decreases and consequently the power of the PV-array is higher than the load demand and the status of the battery changes from discharged to charged instantly (Fig.
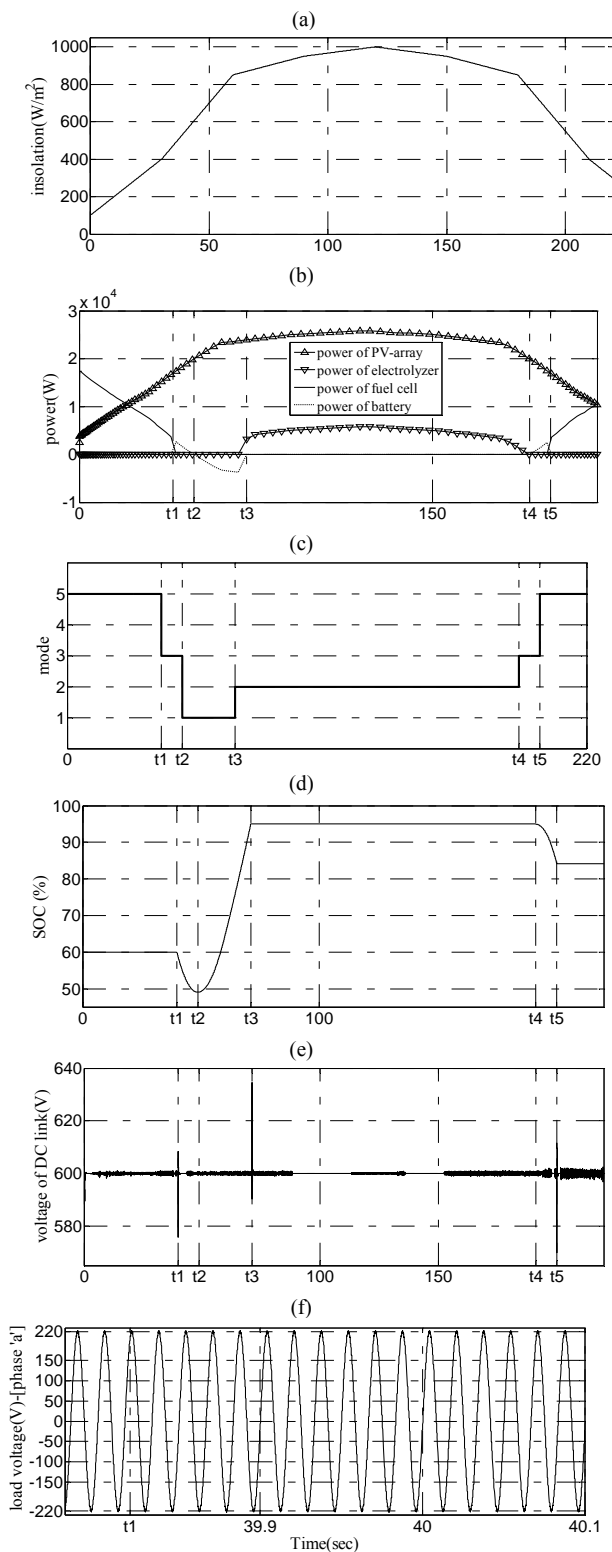
Figure 5 Dynamic response of the system in scenario I, (a) insolation pattern, (b) power of DG units, (c) operating modes of the system, (d) SOC of the battery, (e) DC link voltage, (f) phase *a* voltage of the load

6(c)). After t_4=53.25s, when the battery voltage reaches $V_{bat,max}$, the electrolyzer starts to take the exceeding power, which is higher than the scenario I due to the decreasing of the load demand. Fig. 6(d) shows the DC link voltage in the vicinity of the load change time which is regulated properly after load change by the controllers of DC-DC converters. Fig. 6(e) shows that the load voltage in the vicinity of load change. As it is shown, the AC side controller regulates the load voltage properly after the load.
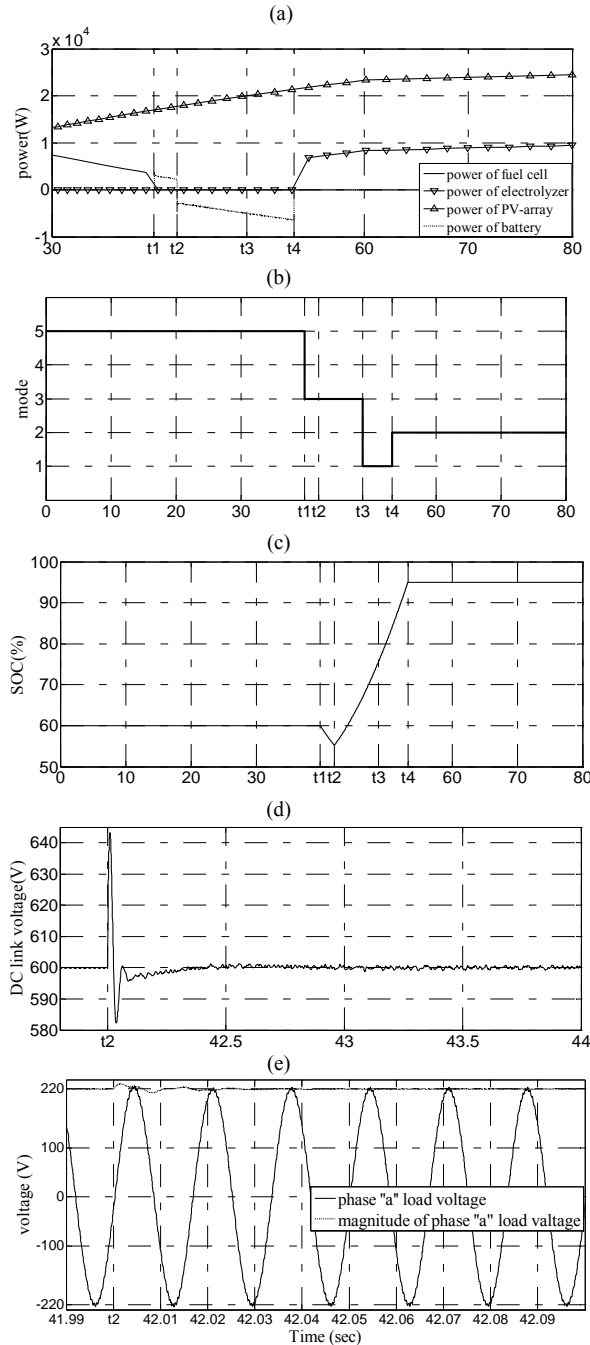
Figure 6   Dynamic response of the system in scenario I, (a) power of DG components, (b) operating modes of the system, (c) SOC of the battery, (d) DC link voltage, and (e) phase *a* voltage of load

VII. CONCLUSIONS

This paper proposes a control strategy for an environmentally friendly stand-alone DG unit system including PV-array, a battery storage, and a hydrogen unit. The units are connected together through DC-DC converters at the DC link of a VSC, which is connected to a three-phase balanced *RLC* load. The DC side control system consists of a supervisory controller and four sub controller associated with each DC-DC converter. The DC side control system manages the power flow between the units and the load as well as maintains the DC link voltage at constant level. The AC side controller regulates the load voltage. The two different scenarios are carried out in MATLAB/Simulink and show usefulness of the proposed control system.

REFERENCES

[1]   H. Patel and V. Agarwal, "Maximum power point tracking scheme for PV systems operating under Partially shaded condition" *IEEE Trans.on Industrial electronics* , vol. 55, NO. 4, April 2008

[2]   W. Shengtie, Q. Zhiyam," Coordination Control of Energy Management for Stand-alone Wind/PV Hybrid systems". *IEEE ICIEA* 2009, pp. 3240 - 3244.

[3]   M. Shirazi, H. Karimi, M. R. Zolghadri, "voltage control of a stand-alone distributed generation system including PV-array and battery storage", accepted for presentation in PEDSTC, Feb 16-17, 2011

[4]   V. M. Pacheco, L. C. Freitas, J. J. B. Viera, E. A. A. Coelho, and V. J. Farias, "A DC-DC converter adequate for alternative supply system application" Proc. *IEEE APEC*, 2002, pp. 1074-1080.

[5]   Wang, C., Nehrir, M.H. Power management of a stand-alone wind/photovoltaic/fuel cell energy system (2008) *IEEE Trans. on Energy Conversion*, 23 (3), pp. 957-967.

[6]   H. Karimi, H. Nikkhajoei, R. Iravani, "Control of an electronically-coupled distributed resource unit subsequent to an islanding event" *IEEE Trans, POWER DELIVERY*, vol. 23, no.1, January 2008.

[7]   Huan-Liang Tsai, Ci-Siang Tu, and Yi-Jie Su "Development of Generelized Photovoltaic Using MATLAB/SIMULINK", *WCECS* 2008, October 22 - 24, 2008,

[8]   Xiao, N. Ozog, W. G. Dunford. "Topology study of photovoltaic interface for maximum power point tracking," *IEEE Trans on Industrial Electronics*, Vol. 54, No. 3, pp. 1696-1704, 2007.

[9]   Y. Sukamongol, S. Chungpaibulpatana and W. Ongsakul,"A simulation model for predicting the performance of a solar photovoltaic system with alternating current loads", Renewable energy, Vol 27, PP. 237-25, October, 2002

[10]   C. Wang, M. H. Nehrir, and S. R. Shaw, "Dynamic models and model validation for PEM fuel cells using electrical circuits," *IEEE Trans. Energy Convers.*, vol. 20, no. 2, pp. 442–451, Jun. 2005.

[11]   Chiara Boccaletti, Gerardo Duni, Gianluca Fabbri, Ezio Santini ,"Simulation Models of Fuel Cell Systems", July 11, 2006.

[12]   Help of Matlab\simulink for fuel cell

[13]   Ke Jin, Xinbo Ruan, Mengxiong Yang, and Min Xu, "A Hybrid Fuel Cell Power System" *IEEE Trans. ON INDUSTRIAL ELECTRONICS*, VOL. 56, NO. 4, APRIL 2009

[14]   R. Gopinath, K. Sangsun, H. Jae-Hong, P. N. Enjeti, M. B. Yeary, and J. W. Howze, "Development of a low cost fuel cell inverter system with DSP control," *IEEE Trans. Power Electron.*, vol. 19, no. 5, pp. 1256–1262, Sep. 2004.

[15]   K. Agbossou, M. Kolhe, J. Hamelin, and T. K. Bose, "Performance of a stand-alone renewable energy system based on energy storage as hydrogen," *IEEE Trans. Energy Convers.*, vol. 19, no. 3, pp. 633–640, Sep. 2004.

[16]   O. Ulleberg, "Modeling of advanced alkaline electrolyzers: a system simulation approach," International Journal of Hydrogen Energy 28 (2003) 21-23.

[17]   Robert W. Erickson, Dragan Maksimovic, "Fundamentals of Power Electronics" (third Edition), chapter 7.